WEARABLE MULTI-SENSOR SYSTEM FOR TELEMEDICINE APPLICATIONS

Ján Hýbl, Petr Volf, Jan Hejda, Aleksei Karavaev, Patrik Kutílek

Faculty of biomedical Engineering, Czech technical university in Prague, Kladno, Czech Republic

Abstract

In this paper, we describe a technical design of wearable multi-sensor systems for physiological data measurement and wide medical applications, significantly impacted in telehealth. The monitors are composed of three analog front-end (AFE) devices, which assist with interfacing digital electronics to the noise-, time-sensitive physiological sensors for measuring ECG (heart-rate monitor), RR (respiration-rate monitor), SRL (skin resistivity monitor). These three types of sensors can be used separately or together and allow to determine a number of parameters for the assessment of mental and physical condition. The system is designed based on requirements for demanding environments even outside the realm of medical applications, and in accordance with Health and Safety at Work directives (89/391/CE and Seveso-II 96/82/EC) for occupational hygiene, medical, rehabilitation, sports and fitness applications.

Keywords

telehealth, physiological sensor, heart-rate, respiration-rate, skin resistivity, monitor

Introduction to telemedicine systems

The miniaturization of electronics makes it possible to produce new wearable devices for sensing biopotentials from the skin surface as well as implantable devices [1]. Miniaturization allows the integration of high-gain, low-noise digitally controllable operational amplifiers along with analog digital converters (ADCs) with up to 32-bit resolution into wearable devices. Progress in smartphone technology leads to increasingly frequent connection with wearable sensors using mobile phone applications (apps) [2–4], or direct integration of sensors into mobile phones [5].

The availability of wearable devices for measuring biopotentials is significantly increasing thanks to the mentioned miniaturization, progress in mobile technology and reduction of production costs [6–7]. Manufacturers such as Apple, Samsung, Garmin offer their devices for home use and within telecare. Their products are usually closed-source and have proprietary operating software that provides aggregated data and calculated parameters. Some manufacturers, e.g., Polar, Empatica offer systems with an SDK or software that provides clean data modified only by bandpass filters. These open devices are suitable for use in telemedicine.

Telemedicine, telehealth, and telecare are terms that refer to a way of delivering healthcare remotely and interactively. The U.S. Federal Communications Commission has defined telemedicine as the use of telecommunications technologies that promotes delivery of all types of medical, diagnostic, and treatment services that are typically provided by physicians (e.g., diagnostic tests, monitoring patient progress after treatment or therapy, access to specialists). Telehealth is similar to telemedicine, but it includes a wider range of remote health services beyond the doctor–patient relationship (e.g., services of nurses, pharmacists and social workers, medication adherence). Telecare generally refers to technology that allows consumers to remain safe and independent in their homes. For example, telecare can include consumer-facing health and fitness apps, sensors and tools that connect consumers with family members or other caregivers, exercise tracking tools, digital medication reminder systems, or early warning and detection technologies [8].

In this paper, we describe an exemplary technical design of a wearable multi-sensor monitors and physiological data measurement system for telemedicine, telehealth, and telecare applications. Thus, the goal of the work is to present a new multisensory telemedicine system that would allow easy application in all areas of research, that would be open to modifications and easily adapted to more extreme conditions of measurement of subjects, e.g., during sports activities, i.e., training of rescuers, sailors, etc. The system reacts to shortcomings of wearable systems described above and should be simpler and more user-friendly.

Lekar a technika – Clinician and Technology 2021, vol. 51(1–4), pp. 76–83, DOI: 10.14311/CTJ.2021.1.12
ISSN 0301-5491 (Print), ISSN 2336-5552 (Online)

Wearable telecare multi-sensor monitor

The described device is based on national utility model no. 34958: ”Monitoring equipment for aggregating biological and physical body data” [9], especially in wearable diagnostic and rehabilitation systems. The essence of which is that it consists of a multisensory system that contains at least two sensors selected from the group:

- body electric potential sensors (EPS) [10],
- bioelectrical impedance sensors (BIS) [11],
- visible spectrum light sensors,
- IR body light sensors,
- sensors of light absorption and scatter in human tissue (plethysmography),
- kinematic and dynamic sensors of body movements physical activity like posture manifestation (accelerometers) or breathing movements (strange gaudes),
- body temperature sensors,
- body audio intensity sensors (phonendoscopy),
- body acoustic impedance sensors (sonography),
- breathing air flow and CO_2 concentration sensors,
- skin surface pH sensors [9].

The sensors or leads are connected to data acquisition and storage unit, see in Fig. 1. The microcontroller (MCU) communicates with each analog front-end (AFE), sets AFE's parameters and receives measured data, which are later synchronized and presented in a form of raw data time series and time series of calculated parameters. The calculated parameters can be chosen to be trivial in the form of simple averaging or advanced using deep neural networks in the form of calculated parameters such as stress, cognitive load, or movement patterns. The possible aggregation types depend on type and number of connected sensors.

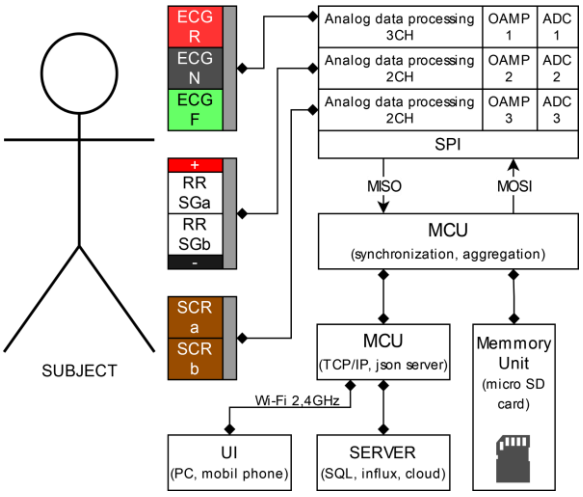

Fig. 1: Data acquisition and storage unit function diagram of the Wearable Telecare Multi-Sensor Monitor.

The wearable multi-sensor monitor described in this paper has been composed of three analog front-end (AFE) devices [12], that measure ECG (heart-rate monitor with ECG leads in Fig. 2 right), RR (respiration-rate monitor in Fig. 2. left), SRL (skin resistivity level monitor). These three sensors can be used separately, like in Fig. 2 or together (connected to one data acquisition and storage unit) using a combination of signal processing, expert system and AI signal processing. The system can provide data for assessing the mental and physical stress of the monitored subject very well used in Health and Safety at Work (89/391/CE [13] and Seveso-II 96/82/EC [14] directives), occupational hygiene, medical, rehabilitation, sports and fitness applications.

Fig. 2: Two pieces of the Wearable Telecare Multi-Sensor Monitors. On the left, the data acquisition and storage unit with a connected sensor for measuring respiratory activity. On the right, the data acquisition and storage unit with cables for ECG chest electrodes.

Heart-rate monitor

The appropriate choice of AFEs is key to the quality of the proposed device. Biosensing AFEs are characterized by low noise, high common-mode rejection-ratio (CMRR) [15, 16], power-supply-rejection-ratio (PSRR) [15, 16], offset rejection, and high input impedance. Low power consumption and tiny sizes are key qualities of a wearable system.

All three AFEs are the ADS1292R multichannel, simultaneous sampling, 24-bit, delta-sigma (ΔΣ) analog-to-digital converters (ADCs) operate at data rates up to 8 kSPS, with a built-in programmable gain amplifier (PGA), input multiplexer per channel that can be independently connected to the internally-generated signals for test, temperature, and lead-off detection [17]. Any configuration of input channels can be selected using multiplexer (MUX) on the input of PGAs. The ADS1292R includes a fully integrated respiration or skin impedance measurement function. The key characteristics of the ADS1292R chip are in Table 1.

The signals from the measuring electrodes RA and LL are fed to the IN1P, IN1N, IN2P, IN2N pins, as illustrated in block diagram in Fig. 3. Pins are internally connected to a DC coupler block with limited bandwidth. The bandwidth of the amplifier PGA1 and PGA2 (Fig. 3) corresponds to the bandwidth of the useful signal, which is then converted to digital form by the ADCs [17]. ADC1 and ADC2 are connected to

Lekar a technika – Clinician and Technology 2021, vol. 51(1–4), pp. 76–83, DOI: 10.14311/CTJ.2021.1.12
ISSN 0301-5491 (Print), ISSN 2336-5552 (Online)

PGA1 and PAGA2 outputs. The RL electrode signal is fed to the RLDIN, RLDINV and RLDOUT pins (Fig. 3). The pins are internally connected to the RLD block (Fig. 3: RLD_AMP and registers RLDxx) [17]. Using RLD is a well-known technique for reducing interference in ECG imaging systems [18]. It is a technique that is very close to the so-called active shielding. It is not necessary to use the RLD electrode when measuring the ECG, but the measured signal will be noisier than without the connected electrode. The Fig. 3 shows the programmable registers like RLD SW block and MUX block.

Table 1: ADS1292R parameters table [17].

Parameter	Value
ADC	24 bit
Sampling frequency	(used 500 Hz) up to 8 ksps
Input-referred noise	1.3 µVPP
Input bias current	200 pA
CMRR	105 dB
Low power	335 µW/channel

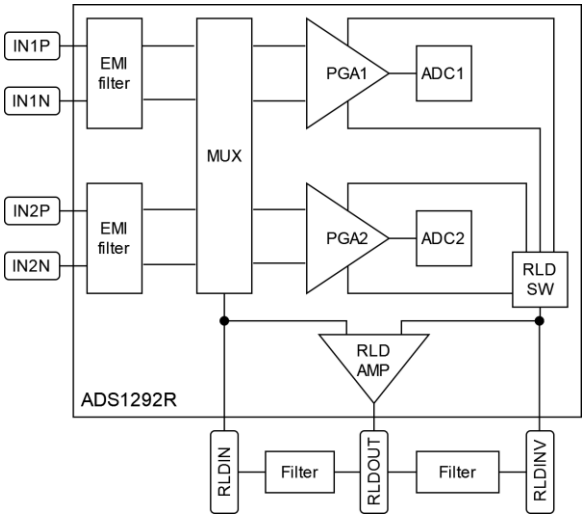

Fig. 3: Example RLD configuration of ADS1292R chip.

Skin resistivity monitor

Bio-impedance is used to estimate various physiochemical and physiological parameters, such as respiration rate, skin hydration level and body composition [19]. There are five basic terms describing bio-impedance. Galvanic skin response (GSR), skin resistance response (SRR), skin conductance response (SCR), skin conductance level (SCL), skin resistance level (SRL) [20, 21].

The proposed device measures bio-impedances in the form of SRL using the two pieces of ADS1292R chip. Each SRL time series is further used to calculate the SRR values, which indicates a momentary fluctuation in skin resistance [20, 21]. The amplitude of the SRL depends on the type and size of the electrodes and distance between them.

An electronic circuit diagram for measuring respiration based on chest SRL [19] and measuring skin conductivity based on SRL was implemented according to the recommendations in technical documentation ADS1292R [17 pg. 62]. The signals from the measuring electrodes RA and LL are also fed through the low pass filter to the RESP_MODP and RESP_MODN pins (Fig. 4). The RESx pins are internally connected to the pneumograph signal demodulator (Fig. 3). Resp Modulator generates a high frequency signal of 32 kHz or 64 kHz frequencies to measure impedance values ranging from 2 kΩ to 15 kΩ [17 pg. 63]. In the described solution the signal was set to 32 kHz with noise levels of less than 7 µV.

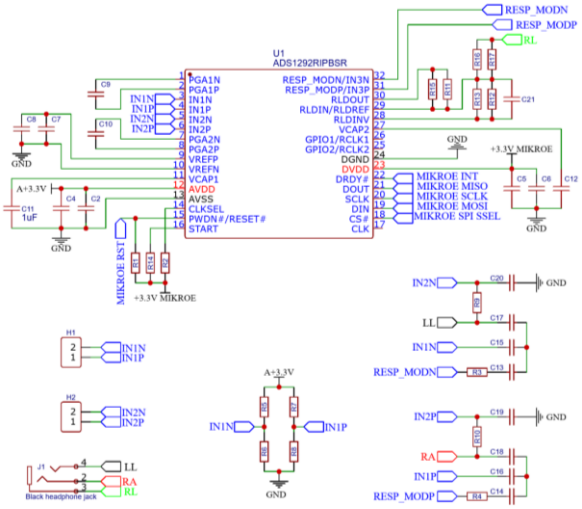

Fig. 4: The ADS1292R universal electric circuit diagram for respiration-rate, heart-rate and skin resistivity monitors.

Respiration-rate monitor

The device provides two respiratory rate sensors, one operating on the principle of mechanical change of the chest volume and the other on the principle of chest bioimpedance using the same leads as the ECG sensor. Second sensor is described in detail in chapter Skin resistivity monitor. First sensor uses a single point load cell (strain gauge force sensor) with a sensitivity of 1.0 mV / V ± 0.15 mV / V with zero output: ± 0.1 mV / V in the measuring range of 1 kg, which converts the force caused by changing the volume of the chest into an electrical quantity. The conversion is performed by strain gauges, which are located on to the sensor body.

Measuring marks change their electrical resistance with a change in their length. The wiring of the measuring marks is shown in Fig. 5. The measuring foil marks are connected to the full measuring bridge and placed along the measuring profile. The bridge is connected to the sensing electronics by four data wires of standardized shielded audio cable with 3.5-mm Jack

Lekar a technika – Clinician and Technology 2021, vol. 51(1–4), pp. 76–83, DOI: 10.14311/CTJ.2021.1.12
ISSN 0301-5491 (Print), ISSN 2336-5552 (Online)

male connector. The red Input(+) and black Input(-) wires supply the bridge by 3.3 V and the white Output(-) and green Output(+) wires form a differential pair connected to the ADS1292R input (Fig. 5 and Fig. 6).

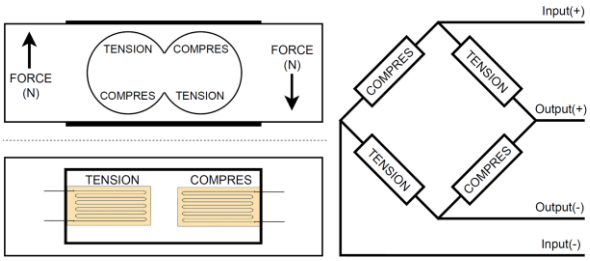

Fig. 5: The single point load cell with 4 foil strain gauge force sensors in full bridge connection [22].

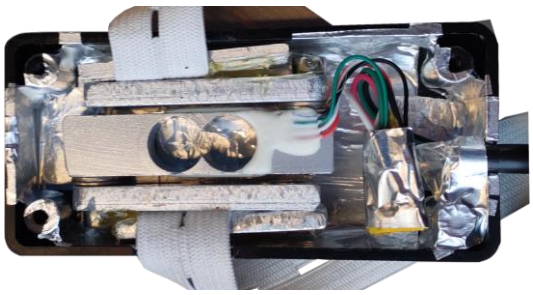

Fig. 6: The single point load cell with an aluminium foil EMI shield and force belt connected in the direction of the force on the sensor, see Fig. 5.

Strain gauge force sensors change resistance as their length changes on the aluminium profile due to the applied deformation force. The measuring bridge output impedance is 1000 Ω ± 10%, dimensions of the sensor in the protection box are 80×35×20 mm (Fig. 6), weight of the sensor and a belt is 100 g.

In the research, we used two different placement methods of single point load cell. Their advantages and disadvantages are described in the discussion.

Wireless communication technology

The use of wireless technology for communication between smaller devices and computers or just between devices, which is often named Internet of Things (IoT) [2, 23], makes these systems more usable. Examples of such wireless technologies are Bluetooth, GSM [4], Zigbee [4], GPRS [4], NB-Iot [23], Wi-Fi. Every mentioned technology has its own user cases, and its own advantages and disadvantages. For example, Bluetooth has a smaller range [4], GPRS has higher communication costs [4] and Wi-Fi has higher power consumption.

Wireless connectivity is provided on the IEEE 802.11 standard (Wi-Fi 2.4 GHz). The communication protocol which is used for transferring data between the device and the application on the PC side is MODBUS TCP. Which is based on point-to-multipoint (P2MP) model, where the server uses a protocol to access a sensor or many sensors and download data from. Each device has its own unique address and gets an IP address from the DHCP server. The PC application has access to all sensors on a local network. The ESP32 chip was chosen as the communication chip and in our case is used as a part of standard ESP32-WROOM-32 development board with internal on-board PCB antenna. Wi-Fi SSID and password is easily set by ESP-TOUCH protocol which implements the Smart Config technology compatible with many smartphone applications. ESP-TOUCH configuration button is accessible for the device user.

Power management and accumulators

Power management and the entire design of the device is based around standardized design of a portable battery source with integrated charging circuit, circuit to protect batteries against discharge. It also provides DC–DC boost circuit to 5 V for USB power standard, DC–DC buck circuit to 3.3 V for MCUs, 3.3 V dropout linear stabilizer for AFE ADS1292R circuits, and light signaling of battery level status. The built-in power supply consists of two 3.7-V 18650 Li-Ion batteries with a total capacity of 6 Ah. For external power supply and charging, it is possible to use standardized USB charging / power supply circuits for portable devices with a voltage range of 5 V. The current consumption of electronics with connected sensors and Wi-Fi interface is up to 250 mA which allows a maximum endurance of 24 hours with fully charged batteries. The standardized enclosure has an aluminum alloy body and is suitable for an indoors standard environment according to ČSN 33 2000-4-41, with a degree of protection IP5x. Operating and storage temperatures are limited by batteries which have operating temperature range from –20 to 65 °C. The device weight is up to 100 g depending on HW configuration and battery size.

PCB design and compatibility

The ADS1292R universal PCB for respiration-rate, heart-rate and skin resistivity monitors was wired according to the datasheet [17 pg. 62] and designed to be compatible with mikroBUS interface, created by MikroElektronika d.o.o. This feature allows a wide application of the designed sensor module. MikroBUS standard board size detail is in Fig. 7 and circuit connection in Fig. 8. The PCB contains all components for impedance measurement on PGA1 (IN1P, IN1N). Alternatively, the PGA1 channel can be used to measure the voltage for the ECG. If the board is used for ECG sensing, the 3.5mm Jack male audio connector can be used to connect the ECG leads and measure the respiration rate and ECG signal simultaneously. The PCB is compatible with MikroElektronika. Add-on board has a standard size S with dimensions 25.4×28.6 mm.

Lekar a technika – Clinician and Technology 2021, vol. 51(1–4), pp. 76–83, DOI: 10.14311/CTJ.2021.1.12
ISSN 0301-5491 (Print), ISSN 2336-5552 (Online)

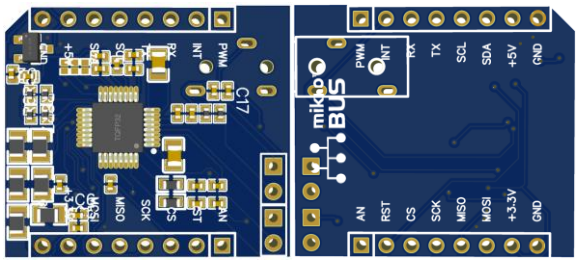

Fig. 7: Top and bottom universal PCB with ADS1292R chip for respiration-rate, heart-rate and skin resistivity monitors.

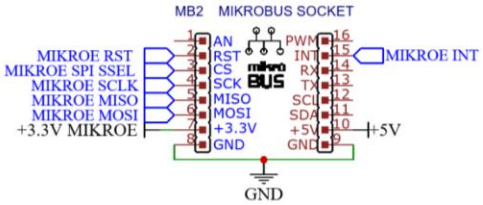

Fig. 8: MikroBUS socket compatible with MikroElektronika's development boards.

Results

The wearable telecare multi-sensor monitor was designed to allow cognitive load measurement using sensors with following technical specification:

- 1 CH ECG sensor with R-R interval detector and sample frequency 500 Hz. The IEC electrodes color standard was used.
- Mechanical respiration rate sensor with sampling frequency 125 Hz.
- SRL sensor with Ohm output and sampling frequency 125 Hz.

Measuring application on the PC side was designed in Python language and acts like a TCP MODBUS client. The client calls the server every one second, receives the contents of the buffer, reads the data (see Table 2) and binds them with timestamps to the already received data into an asynchronous FIFO buffer, which is used for continuous real-time data processing and plotting in graphs or for saving to HDF5 or CSV files.

Table 2: Sample values of the Wearable Telehealth Multi-Sensor Monitor in csv file in SD card.

Column Name	Data example
Time (ms)	1.64025E+12
rawData_bodyBioimpedance (kOhm)	1.507
rawData_ECG (mV)	1.494
rawData_handBioimpedance (kOhm)	1.230
rawData_tenzo (mV)	7.506

Discussion

The wearable telecare multi-sensor monitor was assembled from several functional modules. The fabrication of the mentioned device is time-inefficient and costly due to the difficult connection of several PCBs using wires. The goal of further development is to miniaturize the electronics further and create a complex platform that incorporates AFE circuits, ADC circuits, communication circuits, power management circuits, and user interface circuits in the form of buttons and indication LEDs.

The custom PCB will allow better distribution of data and power paths to the individual PCB layers, better shielding of signal paths, better distribution of power elements, design of more accurate filters for the measured signal bands, more significant separation of the digital electronics and analog electronics power supplies thus reducing noise and increasing PSRR, elimination of DC–DC boost and buck circuits. Further, the electronics and single PCB will rapidly reduce manufacturing time and cost.

During development we had several problems with cable colors in Jack cables packs. Many manufacturers of these cables supply the cable with their own color coding or only text marking, Fig. 2. In the end, we had to have our own cable sets made with the correct colors, see Table 3.

Table 3: Color coding of the ECG leads.

Body Location	AHA Inscription - Color	IEC Inscription - Color
Right Arm	RA - White	R - Red
Left Leg	LL - Red	N - Black
Right Leg	RL - Green	F - Green

AHA—American Heart Association.
IEC — International Electrotechnical Commission.

Wi-Fi communication technology, mentioned in chapter Wireless communication technology, has the disadvantage of high-power consumption (100 to 250 mA) but the advantage of high data rates, long signal range, and good availability of the technology in businesses, healthcare, and households.

During the device design, we focused on testing the breath sensors technology based on strain gauge weighing sensors [24, 25]. The first scenario was the use of direct foil strain gauges. In this case, however, we would have to choose suitable deformation materials, on which they then glue the marks and insulate them with sealants for a longer life of the sensor created in this way. Due to the high workload, we decided to use easily available and cheap scale sensors for personal and business use. A detailed

Lekar a technika – Clinician and Technology 2021, vol. 51(1–4), pp. 76–83, DOI: 10.14311/CTJ.2021.1.12
ISSN 0301-5491 (Print), ISSN 2336-5552 (Online)

description of the technology is in the article Fabrication and Validation of Respiratory Control Belt Using Load Cell Sensor [25]. The advantage of the weight sensor is the linear dependence of the voltage output on input load, publicly available calibration curve and the specified accuracy. The first variant of the strain gauge belt had a sensor positioned so that the force vector acted along the strain gauges, i.e., the rubber band emanated from the longitudinal ends of the strain gauge sensor, as shown in Fig. 9. The sensor was placed incorrectly from the construction point of view, nevertheless it allows for more internal free space and easier and quicker installation. Even so, the sensor achieved sufficient voltage changes for the sensitive electronics to obtain data and construct respiratory activity curves. The breath curve is constructed based on relative change in force and is represented by voltage over time with compensated bias. In this case, the information on the specific absolute value of the force could not be read.

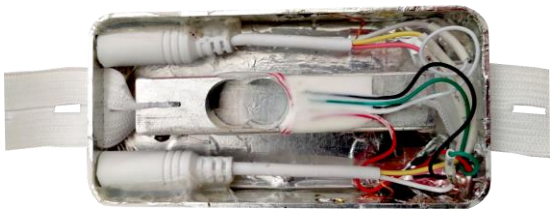

Fig. 9: Strain gauge force sensor with an aluminium foil protecting sensitive electronics from electro-magnetic interference.

The next step in the development was to test the different belt configuration, which had the sensor positioned correctly, so the strain gauges are perpendicular to the direction of the force and are stressed to shear. It was also necessary to make aluminum clamping elements screwed on both sides of the sensor body, as shown in Fig. 8. The sensor manufactured in this way has a larger gain and what is more important the measured voltage change corresponds directly to the force acting on the sensor according to the calibration curve.

The main benefit of knowing the absolute value of the force acting on the breath sensor is the ability to monitor how strongly the belt is tightened on the chest. This information is used in the case of repeated installation of the belt on one subject, as a differently tightened belt has an effect on the breath cycle.

Furthermore, the absolute value of the force is used to monitor how tightly the belt is tightened. If the belt is not tightened, the quality of the recording will be reduced, the movement artifacts will be more visible, and the breath belt may come loose during the next breathing cycle. The quality of the recording may not be poor at first glance, as the relative change in force acting on the breath belt as the chest volume changes is used to plot the breath curve. The combined system using both absolute and relative changes over time informs the operator or user about the possibility of reduced signal quality and thus the fidelity of the interpretation of breathing activity data.

The last advantage of knowing the absolute tightening force of the belt is the prevention of bruises. We plan to use the belts for long-term monitoring of vital signs (weeks to months). Too tight a belt could put pressure on the skin and cause skin irritation or tissue damage [26, 27]. Skin irritation can have a negative effect on the subject's performance and increase the number of artifacts in the measured signal.

The tested technology has proved its worth both in terms of the quality of the provided data, and in terms of price and complexity of technical implementation compared to, for example, the use of Piezoresistive Array [28].

Conclusion

The wearable telecare multi-sensor monitor was designed to be able to perform cognitive load measurement configuration with three sensors. The device has been used to measure physiological data within the research projects "Enhancing Robotic Physiotherapeutic Treatment using Machine Learning" and "Tool for assessment of personal characteristics and external factors to improve efficiency and collaboration of the team during a long-time stay in ICE". Follow-up work is devoted to the evaluation and processing of measured data. In this paper, the parameters of the proposed device, technical details, and physical principles on which the device works were described in detail.

The wearable telecare multi-sensor monitor will be used for the collection and evaluation of physiological data in order to design algorithms for automated evaluation of cognitive and stress load of individuals and work teams with future use as a measurement device to support the improvement of safety and health of employees at work in harmonization with directives Seveso-III (Directive 2012/18/EU) or upper named directive Seveso-II and Council Directive 89/391/EEC of 12 June 1989 on the introduction of measures to encourage improvements in the safety and health of workers at work.

Conflict of Interest

None to report.

Acknowledgement

The research has been supported by the Ministry of Science & Technology, Israel and The Ministry of

Lekar a technika – Clinician and Technology 2021, vol. 51(1–4), pp. 76–83, DOI: 10.14311/CTJ.2021.1.12
ISSN 0301-5491 (Print), ISSN 2336-5552 (Online)

Education, Youth and Sports of the Czech Republic in a research grant no. LTAIZ19008, Enhancing Robotic Physiotherapeutic Treatment using Machine Learning. The research has been supported by a research grant of the Technology Agency of the Czech Republic no. TL05000228.

A preliminary version of the results published in this article was presented at the Trends in Biomedical Engineering 2021 conference.

References

[1] Kim J, Kim H, Kim D, Park HJ, Ban K, Ahn S, et al. A wireless power transfer based implantable ECG monitoring device. Energies. 2020 Feb 18;13(4):905. DOI: 10.3390/en13040905

[2] Nornaim MH, Abdul-Kadir NA, Harun FK, Razak MA. A Wireless ECG Device with Mobile Applications for Android. In: 2020 7th International Conference on Electrical Engineering, Computer Sciences and Informatics (EECSI); 2020 Oct 1–2; Yogyakarta, Indonesia. IEEE; 2020 Nov 12. pp. 168–71. DOI: 10.23919/EECSI50503.2020.9251871

[3] Liu L, Liu J. Biomedical sensor technologies on the platform of mobile phones. Front Mech Eng. 2011 Apr 29;6:160–75. DOI: 10.1007/s11465-011-0216-0

[4] Ahmed AS, Rijab KS, Alagha SA. Heart Rate and ECG Wireless Monitoring Techniques: A Survey. DJES. 2020 Jun 1;13(2):50–8. DOI: 10.24237/djes.2020.13207

[5] Stankevich E, Paramonov I, Timofeev I. Mobile phone sensors in health applications. In: 2012 12th Conference of Open Innovations Association (FRUCT); 2012 Nov 5–9; Oulu, Finland. IEEE; pp. 1–6. DOI: 10.23919/FRUCT.2012.8122097

[6] Allied Market Research. Wearable Sensors Market Global Opportunities Analysis and Industry Forecast By 2030 [Internet]. Allied Market Research; 2022 [cited 2022 Nov 22]. Available from: https://www.alliedmarketresearch.com/wearable-sensor-market

[7] Precedence Research. Wearable Sensors Market-Global Industry Analysis, Size, Share, Growth, Trends, Regional Outlook, and Forecast 2022-2030 [Internet]. Precedence Research; 2022. [cited 2022 Nov 22]. Available from: https://www.precedenceresearch.com/wearable-sensors-market

[8] Federal Communications Commission. Telehealth, Telemedicine, and Telecare: What's What? [Internet]. USA: Federal Communications Commission [reviewed 2022 Nov 19; cited 2022 Nov 19]. Available from: https://www.fcc.gov/general/telehealth-telemedicine-and-telecare-whats-what

[9] Hybl J, Kutílek P, Volf P, Hejda J, Karavaev A; Czech Technical University in Prague. Monitoring equipment for aggregating biological and physical body data. Czech Republic National utility model application CZ 2020-38089. 2021 Mar 30. Available from: https://isdv.upv.cz/webapp/resdb.print_detail.det?pspis=PUV/38089&plang=EN

[10] Pouryazdan A, Prance RJ, Prance H, Roggen D. Wearable electric potential sensing: A new modality sensing hair touch and restless leg movement. In: Proceedings of the 2016 ACM international joint conference on pervasive and ubiquitous computing: Adjunct; 2016 Sep 12–16; Heidelberg, Germany. New York, NY, USA: Association for Computing Machinery; 2016 Sep 12. pp. 846–50. DOI:10.1145/2968219.2968286

[11] Jung MH, Namkoong K, Lee Y, Koh YJ, Eom K, Jang H, Jung W, Bae J, Park J. Wrist-wearable bioelectrical impedance analyzer with miniature electrodes for daily obesity management. Sci Rep. 2021 Jan 13;11(1):1238. DOI: 10.1038/s41598-020-79667-3

[12] Bhamra H, Lynch J, Ward M, Irazoqui P. A noise-power-area optimized biosensing front end for wireless body sensor nodes and medical implantable devices. IEEE Trans Very Large Scale Integr (VLSI) Syst. 2017 Jun 27;25(10):2917–28. DOI: 10.1109/TVLSI.2017.2714171

[13] Council Directive 89/391/EEC of the 12th June 1989 on the introduction of measures to encourage improvements in the health and of safety workers at work; OJ L 183/1; 1989 Jun 29. Available from: https://eur-lex.europa.eu/eli/dir/1989/391/oj

[14] Council Directive 96/82/EC of 9 December 1996 on the control of major-accident hazards involving dangerous substances; OJ L 10/1; 1997 Jan 14. Available from: https://eur-lex.europa.eu/legal-content/EN/TXT/PDF/?uri=CELEX:01996L0082-20120813&from=EN

[15] Zeng L, Liu B, Heng CH. A dual-loop eight-channel ECG recording system with fast settling mode for 12-lead applications. IEEE J Solid-State Circuits. 2019 Mar 26;54(7):1895–906. DOI: 10.1109/JSSC.2019.2903471

[16] Xiu L, Li Z. Low-power instrumentation amplifier IC design for ECG system applications. Procedia Eng. 2012 Jan 1;29:1533–8. DOI: 10.1016/j.proeng.2012.01.168

[17] Texas Instruments Incorporated. ADS129x Low-Power, 2-Channel, 24-Bit Analog Front-End for Biopotential Measurements (Rev. C) [Data Sheet]. 2011 Dec [revised 2020 Apr; cited 2022 Nov 22]. Available from: https://www.ti.com/product/ADS1292R

[18] Guermandi M, Scarselli EF, Guerrieri R. A Driving Right Leg Circuit (DgRL) for Improved Common Mode Rejection in Bio-Potential Acquisition Systems. IEEE Trans Biomed Circuits Syst. 2015 Aug 14;10(2):507–17. DOI: 10.1109/TBCAS.2015.2446753

[19] Xu J, Harpe P, Pettine J, Van Hoof C, Yazicioglu RF. A low power configurable bio-impedance spectroscopy (BIS) ASIC with simultaneous ECG and respiration recording functionality. In: ESSCIRC Conference 2015 - 41st European Solid-State Circuits Conference (ESSCIRC); 2015 Sep 14–18; Graz, Austria. IEEE; 2015 Nov 2. pp. 396–9. DOI: 10.1109/ESSCIRC.2015.7313911

[20] Lykken DT, Venables PH. Direct measurement of skin conductance: a proposal for standardization. Psychophysiology. 1971 Sep;8(5):656–72. DOI: 10.1111/j.1469-8986.1971.tb00501.x

[21] Edelberg R. The effects of initial levels of sweat duct filling and skin hydration on electrodermal response amplitude. Psychophysiology. 1983 Sep;20(5):550–7. DOI: 10.1111/j.1469-8986.1983.tb03012.x

[22] Marchida, A., Sullivan T., Palladino J. Load Cell Design Using COMSOL Multiphysics. In: Proceedings of the 2012 COMSOL Conference; 2012 Oct 3–5; Newton, MA, USA. Comsol; 2012. Corpus ID: 55708683.

[23] Basu SS, Haxhibeqiri J, Baert M, Moons B, Karaagac A, Crombez P, Camerlynck P, Hoebeke J. An End-To-End LwM2M-Based Communication Architecture for Multimodal NB-IoT/BLE Devices. Sensors (Basel). 2020 Apr 15;20(8):2239. DOI: 10.3390/s20082239

[24] Khatami AA, Mukhtar H, Rahmawati D. Performance Comparison of Strain Sensors for Wearable Device in Respiratory Rate Monitoring. In: Proceedings of the 1st International Conference on Electronics, Biomedical Engineering, and Health Informatics; 2021 Oct 8–9; Surabaya, Indonesia. Singapore: Springer; c2021. pp. 723–34. DOI: 10.1007/978-981-33-6926-9_63

[25] Dallal ZT, Gholami S, Barough MS. Fabrication and Validation of Respiratory Control Belt Using Load Cell Sensor. Front Biomed Technol. 2020 Dec 30;7(4):281–5. DOI: 10.18502/fbt.v7i4.5325

[26] Polley C, Jayarathna T, Gunawardana U, Naik G, Hamilton T, Andreozzi E, Bifulco P, Esposito D, Centracchio J, Gargiulo G. Wearable Bluetooth Triage Healthcare Monitoring System. Sensors (Basel). 2021 Nov 15;21(22):7586 DOI: 10.3390/s21227586

[27] Sunwoo SH, Ha KH, Lee S, Lu N, Kim DH. Wearable and Implantable Soft Bioelectronics: Device Designs and Material Strategies. Annu Rev Chem Biomol Eng. 2021 Jun 7;12:359–91. DOI: 10.1146/annurev-chembioeng-101420-024336

[28] Wang R, Zhang Y, Chen X, Lin F, He R, Lv R, et al. Chest and Abdomen Respiratory Monitoring by Large Area Piezoresistive Array. In: 2021 IEEE International Conference on Flexible and Printable Sensors and Systems (FLEPS); 2021 Jun 20–23; Manchester, United Kingdom. IEEE; 2021 Jul 5. pp. 1–4. DOI: 10.1109/FLEPS51544.2021.9469838

Bc. Ján Hýbl
Department of Health Care and Population Protection
Faculty of Biomedical Engineering
Czech Technical University in Prague
nám. Sítná 3105, CZ-272 01 Kladno

E-mail: jan.hybl@fbmi.cvut.cz
Phone: +420 777 086 473